

## Inclusion Complexes of Cyclodextrins with Benzo[*c*]cinnoline, Phenanthridine, and Phenanthrene in Aqueous Solution Containing an Organic Ion Having a Long Alkyl Chain

Sanyo Hamai

Department of Chemistry, Faculty of Education and Human Studies, Akita University,  
1-1 Tegata Gakuen-machi, Akita 010-8502

Received October 19, 2010; E-mail: hamai@ipc.akita-u.ac.jp

In aqueous solution,  $\gamma$ -CD forms a 1:1 inclusion complex with phenanthrene analogs (phenanthrene (Phen), phenanthridine (Phent), and benzo[*c*]cinnoline (Bcc)). The equilibrium constants,  $K_1$ , for the formation of the 1:1 inclusion complex for the phenanthrene analogs have been evaluated from the fluorescence intensity change. The  $K_1$  values for the phenanthrene analogs are in the range from 100 to 150 mol<sup>-1</sup> dm<sup>3</sup>. The 1:1 inclusion complexes further associate with an alkyltrimethylammonium cation (alkyl sulfate or alkanesulfonate) to form a 1:1:1  $\gamma$ -CD–phenanthrene analog–alkyltrimethylammonium cation (alkyl sulfate or alkanesulfonate) inclusion complex. The equilibrium constants,  $K_2$ , for the formation of the 1:1:1 inclusion complex have been evaluated from a simulation for the fluorescence intensity change. The  $K_2$  value for the same alkyltrimethylammonium cation is decreased on going from Phen to Bcc. The  $K_2$  value of the phenanthrene analog is increased with the alkyl chain length of the alkyltrimethylammonium cation (alkyl sulfate or alkanesulfonate). In the case of Phen, the  $K_2$  value for an alkyltrimethylammonium cation is less than that for alkyl sulfate or alkanesulfonate having the same alkyl group as the alkyltrimethylammonium cation.

Cyclodextrins (CDs) are cyclic oligosaccharides composed of more than five D-glucopyranose residues.<sup>1,2</sup> Commercially available CDs having six, seven, and eight D-glucopyranose residues are called  $\alpha$ -,  $\beta$ -, and  $\gamma$ -CD, respectively. Because CD has a relatively hydrophobic cavity, it accommodates an organic molecule of appropriate dimensions to form an inclusion complex. Usually, a CD molecule accommodates a single guest molecule to form a 1:1 inclusion complex.<sup>3</sup> In some cases, however, the CD cavity includes the same or different kind of guest molecule to form a 1:2 CD–guest or 1:1:1 CD–guest 1–guest 2 inclusion complex.<sup>4–10</sup> Previously, we have examined the formation of ternary inclusion complexes of  $\gamma$ -CD with sodium 1-pyrenesulfonate and an organic ion having a long alkyl chain such as trimethyloctylammonium bromide (or sodium 1-dodecyl sulfate).<sup>11</sup> In a dilute solution of 1-pyrenesulfonate,  $\gamma$ -CD forms a 1:1 inclusion complex with 1-pyrenesulfonate. The  $\gamma$ -CD cavity, into which a 1-pyrenesulfonate molecule is incorporated, further accommodates a long alkyl chain of an organic ion such as trimethyloctylammonium bromide to form a 1:1:1 inclusion complexes of  $\gamma$ -CD with 1-pyrenesulfonate and the organic ion.

There have been many studies of inclusion complexes of CD with heterocyclic compounds such as indole derivatives.<sup>12–16</sup> Heterocyclic compounds may exhibit behavior different from a parent aromatic hydrocarbon toward the formation of inclusion complexes with CDs, depending on the position and number of heteroatoms. In the case of benzoquinolines, the position of a nitrogen atom on the three fused benzene rings likely affects the interactions with CDs. In a previous paper, we have reported the inclusion interactions of three benzoquinoline isomers with CDs.<sup>17</sup>  $\gamma$ -CD forms 1:1 inclusion complexes with

benzo[*f*]quinoline and phenanthridine, while a benzo[*h*]quinoline solution becomes turbid in the presence of  $\gamma$ -CD. Excimer fluorescence has been observed from the 2:2  $\gamma$ -CD–benzo[*f*]quinoline inclusion complex, which is formed by the association of 1:1  $\gamma$ -CD–benzo[*f*]quinoline inclusion complexes. In addition to the difference in the magnitude of an equilibrium constant for the formation of the 1:1 inclusion complex of CD, the 1:1 inclusion complexes of benzo[*f*]quinoline and phenanthridine behave differently toward their association. For the benzoquinolines, a ternary inclusion complex of  $\gamma$ -CD with alcohol such as 1-pentanol has not been observed, although a 1:1:1 inclusion complex of  $\gamma$ -CD with propylene oxide (or tetrahydrofuran) has been observed. Taking into account the diverse inclusion behavior of the benzoquinoline isomers, a heterocyclic compound is expected to differently behave with respect to the inclusion interactions with CD, compared to a parent aromatic hydrocarbon. To our knowledge however, there has been no study on the effects of the presence of a heteroatom on an aromatic ring in forming an inclusion complex with CD.

In a series of studies on the formation of ternary inclusion complexes of CDs, we have been interested in whether or not a ternary inclusion complex is formed or not among CD, a heterocyclic compound, and an organic ion having a long alkyl chain, although CD forms a ternary inclusion complex with a heterocyclic compound and neutral alcohol (or ether).<sup>16,17</sup> Surfactants, which have both a hydrophobic moiety and a hydrophilic moiety within a single molecule, are used in various fields, because surfactants affect the surface tension of solution and form micelles at high concentrations. A long alkyl chain is responsible for the hydrophobicity of cationic or anionic surfactants. Consequently, it is valuable to examine the

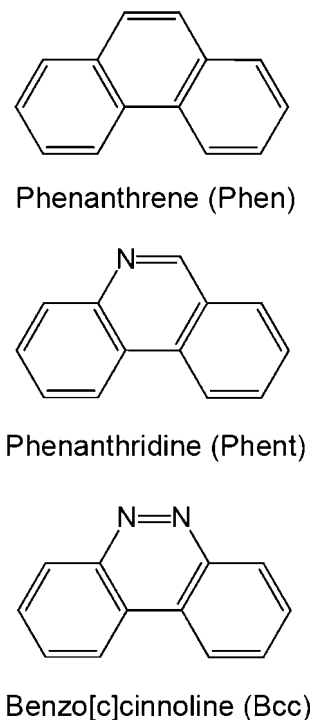


Chart 1.

interactions of surfactants with long alkyl chains with a guest molecule in ternary inclusion complexes of CD. When the ternary inclusion complex of a heterocyclic compound is formed, the effects of a heteroatom on the formation of the inclusion complex may be clarified by a comparison with the inclusion behavior of a parent compound having no heteroatom.

The formation of inclusion complexes of phenanthrene with  $\beta$ - and  $\gamma$ -CDs has been investigated by means of a volatilization-rate method and a fluorescence method.<sup>18,19</sup> Thus, we selected phenanthrene as a parent aromatic hydrocarbon without a heteroatom. Phenanthridine and benzo[c]cinnoline were selected as heterocyclic compounds derived from parent phenanthrene; phenanthridine, and benzo[c]cinnoline have one and two nitrogen atoms on the phenanthrene ring, respectively (Chart 1).

### Experimental

$\gamma$ -Cyclodextrin ( $\gamma$ -CD), which was purchased from Tokyo Chemical Industry Co., Ltd. was used as received.  $\beta$ -Cyclodextrin ( $\beta$ -CD) purchased from Nacalai Tesque, Inc. was twice recrystallized from water. Phenanthrene (Phen) obtained from Tokyo Chemical Industry Co., Ltd. was recrystallized from ethanol. Phenanthridine (Phent) and benzo[c]cinnoline (Bcc), which were purchased from Tokyo Chemical Industry Co., Ltd., were recrystallized from hexane. Trimethyloctylammonium bromide (TMOA), decyltrimethylammonium bromide (DeTMA), dodecyltrimethylammonium chloride (DoTMA), sodium 1-decanesulfonate (SDeS), and sodium 1-undecanesulfonate (SUnS), which were obtained from Tokyo Chemical Industry Co., Ltd., were used as received. Sodium 1-dodecyl sulfate (SDoS) purchased from Nacalai Tesque Inc. was used without further purification.

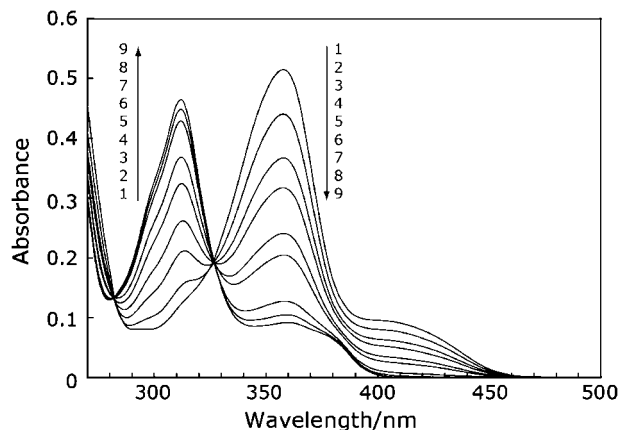


**Figure 1.** Absorption spectra of Bcc ( $4.9 \times 10^{-5} \text{ mol dm}^{-3}$ ) in aqueous solutions of various pH values. pH: (1) 0.83, (2) 1.13, (3) 1.44, (4) 1.74, (5) 2.02, (6) 2.22, (7) 2.77, (8) 3.05, and (9) 4.72.

The concentrations of TMOA, DeTMA, DoTMA, SDeS, SUnS, and SDoS used in this study were less than their critical micelle concentrations, respectively. The concentrations of Phen, Phent, and Bcc were estimated under the assumption that their molar absorption coefficients in water are the same as those in methanol, respectively. Buffers ( $6.7 \times 10^{-4} \text{ mol dm}^{-3}$  of  $\text{KH}_2\text{PO}_4$  and  $2.7 \times 10^{-3} \text{ mol dm}^{-3}$  of  $\text{Na}_2\text{HPO}_4$ ) of pH 7.3 were used for Phent solution.

The fluorescence quantum yields of Bcc were evaluated relative to that of quinine sulfate in  $1.0 \text{ mol dm}^{-3} \text{ H}_2\text{SO}_4$ .<sup>20</sup>

Absorption spectra were recorded on a Shimadzu UV-2450 spectrophotometer. Fluorescence spectra were taken with a Shimadzu RF-501 spectrofluorometer equipped with a cooled Hamamatsu R-943 photomultiplier or a Shimadzu RF-5300 PC spectrofluorophotometer. The fluorescence spectra were corrected for the spectral response of the fluorometers. Spectroscopic measurements were made at  $25 \pm 0.1^\circ \text{C}$ .

### Results and Discussion

**pH Dependence of Absorption and Fluorescence Spectra of Bcc.** Figure 1 shows the pH dependence of the absorption spectrum of Bcc ( $4.9 \times 10^{-5} \text{ mol dm}^{-3}$ ) in aqueous solution. As a pH value of solution is increased from 0.83 to 4.72, an absorption band at 312 nm is increased in intensity, while an absorption bands at 358 and 410 nm are reduced. An isosbestic point is observed at 327 nm. These findings indicate that Bcc is deprotonated in weakly acidic and neutral solution, while it is protonated in strongly acidic solution. From the pH dependence of the absorbance at 358 nm, the  $\text{pK}_a$  value of Bcc has been estimated to be 1.68 (Figure S1). Consequently, Bcc in the ground state exists as a neutral form in aqueous solution without buffer. Figure 2 shows fluorescence spectra of Bcc ( $2.5 \times 10^{-5} \text{ mol dm}^{-3}$ ) in solutions of various pHs. When a pH value is increased from 0.83 to 2.02, the fluorescence is enhanced. As the pH value is further increased, the fluorescence intensity is conversely decreased, accompanied by a slight peak shift to shorter wavelengths. Because Bcc has two nitrogen atoms, the pH dependence of the fluorescence spectrum shows two-step protonation. Figure 3 depicts the pH dependence of the fluorescence intensity at 490 nm. From

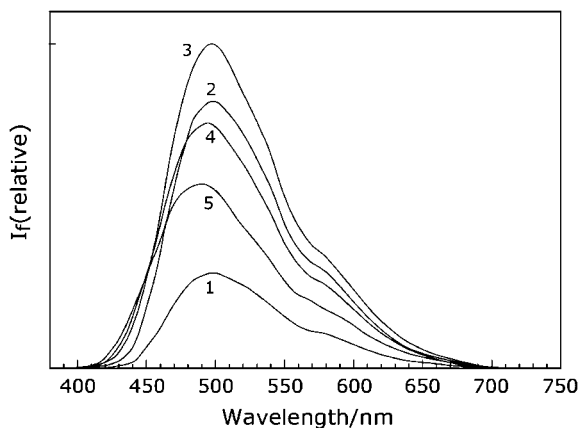


**Figure 2.** Fluorescence spectra of Bcc ( $2.5 \times 10^{-5} \text{ mol dm}^{-3}$ ) in aqueous solutions of various pH values. pH: (1) 0.83, (2) 1.44, (3) 2.02, (4) 2.74, and (5) 4.72.  $\lambda_{\text{ex}} = 327 \text{ nm}$ .

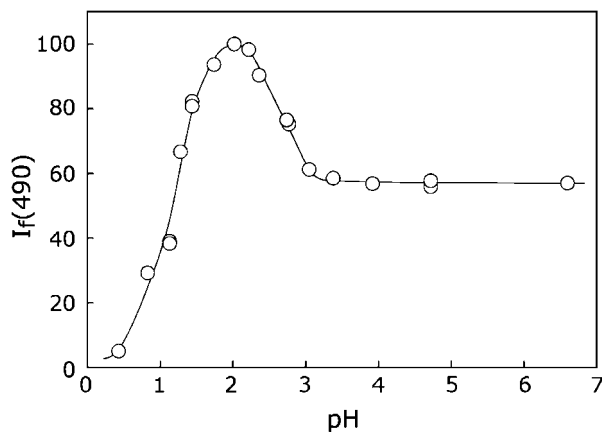


**Figure 3.** pH dependence of the fluorescence intensity of Bcc observed at 490 nm. The maximum fluorescence intensity is normalized to 100.  $[\text{Bcc}] = 2.5 \times 10^{-5} \text{ mol dm}^{-3}$ .  $\lambda_{\text{ex}} = 327 \text{ nm}$ .

this pH dependence, the apparent  $\text{p}K_{\text{a}1}^*$  and  $\text{p}K_{\text{a}2}^*$  values are estimated to be 1.12 and 2.64, respectively. This indicates that in the excited singlet state as well as the ground state, Bcc in aqueous solution exists in a neutral form.

**Inclusion Complex of  $\gamma$ -CD with Bcc.** Figure 4 exhibits absorption spectra of Bcc ( $2.5 \times 10^{-5} \text{ mol dm}^{-3}$ ) in aqueous solution containing various concentrations of  $\gamma$ -CD. When  $\gamma$ -CD is added to Bcc solution, the absorption peak at 312 nm is decreased in intensity, suggesting the formation of an inclusion complex of  $\gamma$ -CD with Bcc. The reason why the intensity of the absorption peak is weakened is not clear at present. Figure 5 shows fluorescence spectra of Bcc ( $2.5 \times 10^{-5} \text{ mol dm}^{-3}$ ) in aqueous solution in the absence and presence of  $\gamma$ -CD ( $1.0 \times 10^{-2} \text{ mol dm}^{-3}$ ). In the presence of  $\gamma$ -CD, the fluorescence intensity is decreased, suggesting the formation of the inclusion complex between  $\gamma$ -CD and Bcc. The decrease in the fluorescence of Bcc by the addition of  $\gamma$ -CD may partly due to the decrease in the absorbance at an excitation wavelength. The fluorescence quantum yields of Bcc in water and cyclohexane have been estimated to be 0.0065 and 0.0050, respectively.

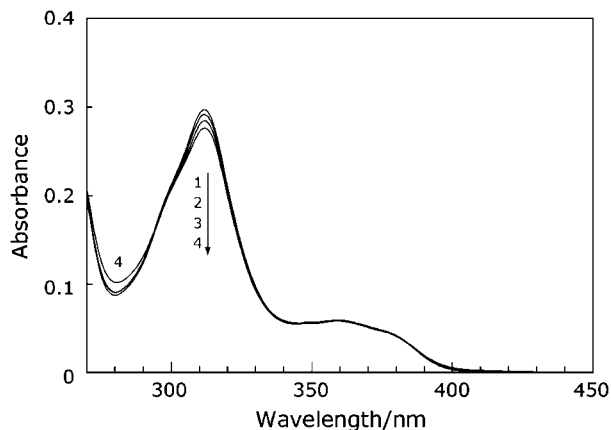


**Figure 4.** Absorption spectra of Bcc ( $2.5 \times 10^{-5} \text{ mol dm}^{-3}$ ) in aqueous solutions containing various concentrations of  $\gamma$ -CD. Concentration of  $\gamma$ -CD: (1) 0, (2)  $1.0 \times 10^{-3}$ , (3)  $3.0 \times 10^{-3}$ , and (4)  $1.0 \times 10^{-2} \text{ mol dm}^{-3}$ .

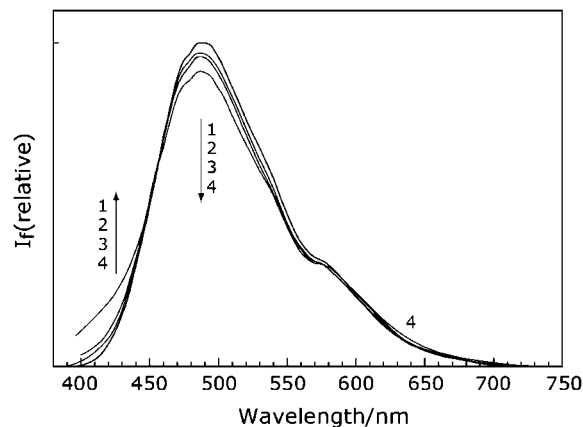


**Figure 5.** Fluorescence spectra of Bcc ( $2.5 \times 10^{-5} \text{ mol dm}^{-3}$ ) in aqueous solutions containing various concentrations of  $\gamma$ -CD. Concentration of  $\gamma$ -CD: (1) 0, (2)  $1.0 \times 10^{-3}$ , (3)  $3.0 \times 10^{-3}$ , and (4)  $1.0 \times 10^{-2} \text{ mol dm}^{-3}$ .  $\lambda_{\text{ex}} = 330 \text{ nm}$ .

In addition to the decrease in the absorbance, therefore, the decrease in the fluorescence intensity may partly be due to the absence of the hydrogen bonding between water and Bcc, which is located within the  $\gamma$ -CD cavity. When the inclusion complex has a 1:1 stoichiometry concerning  $\gamma$ -CD and Bcc, the equation (double reciprocal plot) holds for the fluorescence intensity:<sup>21</sup>

$$1/(I_f - I_f^0) = 1/a + 1/(aK_1[\gamma\text{-CD}]) \quad (1)$$

Here,  $I_f$  and  $I_f^0$  are the fluorescence intensities in the presence and absence of  $\gamma$ -CD, respectively, and  $a$ ,  $K_1$ , and  $[\gamma\text{-CD}]$  are an instrumental constant including the fluorescence quantum yields of free Bcc and the 1:1  $\gamma$ -CD–Bcc inclusion complex, the equilibrium constant for the formation of the 1:1  $\gamma$ -CD–Bcc inclusion complex, and the  $\gamma$ -CD concentration, respectively. Figure 6 shows a double-reciprocal plot for the fluorescence intensity of Bcc ( $2.5 \times 10^{-5} \text{ mol dm}^{-3}$ ) in aqueous solution containing  $\gamma$ -CD. The plot exhibits a straight line, indicating that the  $\gamma$ -CD–Bcc inclusion complex has a 1:1 stoichiometry concerning  $\gamma$ -CD and Bcc.

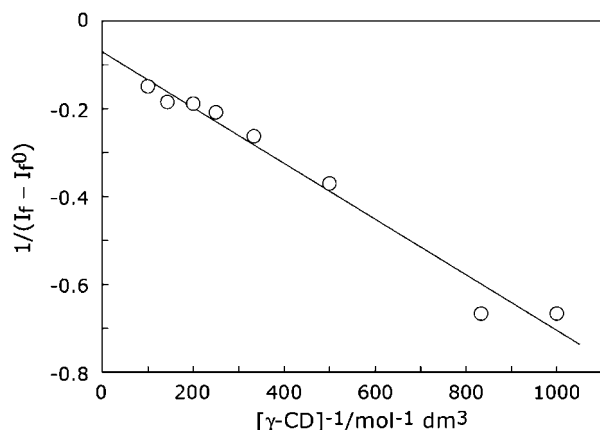
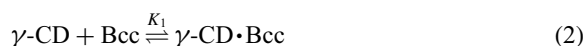


**Figure 6.** Double-reciprocal plot for the fluorescence intensity of Bcc ( $2.5 \times 10^{-5} \text{ mol dm}^{-3}$ ) in aqueous solutions containing  $\gamma$ -CD. A value of a correlation coefficient is  $-0.987$ .  $\lambda_{\text{ex}} = 330 \text{ nm}$ .  $\lambda_{\text{obs}} = 490 \text{ nm}$ .



where  $\gamma\text{-CD} \cdot \text{Bcc}$  is the 1:1  $\gamma\text{-CD}$ –Bcc inclusion complex. From the plot, the  $K_1$  value for the formation of the 1:1  $\gamma\text{-CD}$ –Bcc inclusion complex is evaluated to be  $110 \pm 30 \text{ mol}^{-1} \text{ dm}^3$ , which is less than half of that ( $250 \pm 30 \text{ mol}^{-1} \text{ dm}^3$ ) of benzo[*f*]quinoline and is slightly less than that ( $150 \pm 30 \text{ mol}^{-1} \text{ dm}^3$ ) of phenanthridine.<sup>17</sup> The different numbers of nitrogen atom and the different position of a nitrogen atom(s) are likely responsible for the different  $K_1$  values.

In Figure 5, the longer-wavelength tail is slightly enhanced at a high concentration of  $\gamma$ -CD. This may be due to the excimer fluorescence of Bcc, which is arisen from a 1:2 or 2:2  $\gamma\text{-CD}$ –Bcc inclusion complex.

**Effects of TMOA, DeTMA, and DoTMA on the Formation of Inclusion Complexes of Bcc.** Inclusion complexes are formed between poly(ethylene glycol) and not  $\beta$ -CD but  $\alpha$ -CD.<sup>22</sup> In addition, 1,1'-diheptyl-4,4'-bipyridyl dibromide scarcely forms an inclusion complex with  $\gamma$ -CD, due to the  $\gamma$ -CD cavity being too large to closely include a hydrophobic heptyl chain of 1,1'-diheptyl-4,4'-bipyridyl dibromide.<sup>23</sup> In the presence of  $\gamma$ -CD of  $1.0 \times 10^{-2} \text{ mol dm}^{-3}$ , a change in the conductivity of DoTMA solution is less than 3%, resulting in no evaluation of the equilibrium constant for the formation of an inclusion complex of  $\gamma$ -CD with DoTMA.<sup>11</sup> Consequently, we have neglected the formation of inclusion complexes of  $\gamma$ -CD with organic ions having a long alkyl chain.

The 358-nm absorption band of Bcc in the presence of DeTMA ( $0.005 \text{ mol dm}^{-3}$ ) was slightly decreased by the addition of  $\gamma$ -CD. The spectral change in the 358-nm band may suggest that an inclusion complex is formed among  $\gamma$ -CD, Bcc, and DeTMA. The addition of DeTMA to Bcc solution without  $\gamma$ -CD did not affect the absorption spectrum of Bcc, suggesting no formation of a binary complex of Bcc with DeTMA. However, the absorption bands of Bcc in aqueous solution containing  $\gamma$ -CD ( $3.0 \times 10^{-3} \text{ mol dm}^{-3}$ ) are slightly decreased in intensity by the addition of DeTMA (Figure 7). This finding suggests the formation of the ternary inclusion complex of  $\gamma$ -CD with Bcc and DeTMA.

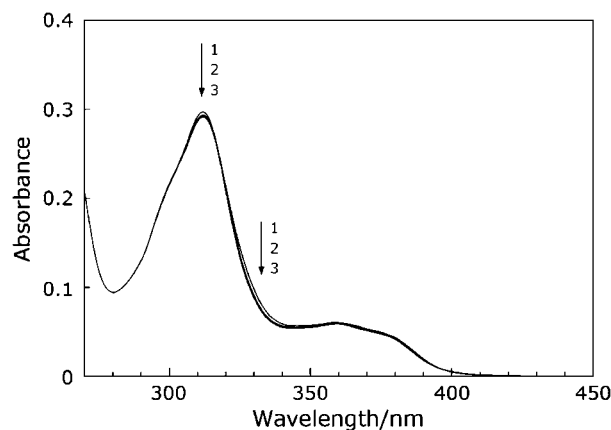
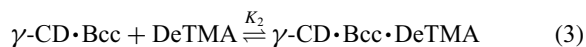


**Figure 7.** Absorption spectra of Bcc ( $2.5 \times 10^{-5} \text{ mol dm}^{-3}$ ) in aqueous solutions containing  $\gamma$ -CD ( $3.0 \times 10^{-3} \text{ mol dm}^{-3}$ ) and several concentrations of DeTMA. Concentration of DeTMA: (1) 0, (2)  $3.0 \times 10^{-3}$ , and (3)  $1.0 \times 10^{-2} \text{ mol dm}^{-3}$ .

As in the case of the fluorescence intensity of Bcc in the absence of DeTMA, the fluorescence intensity in the presence of DeTMA ( $0.01 \text{ mol dm}^{-3}$ ) was reduced as the  $\gamma$ -CD concentration was increased. Taking into account the dimensions of the  $\gamma$ -CD cavity, a Bcc molecule, and a DeTMA molecule, the ternary inclusion complex most likely has a 1:1:1 stoichiometry concerning  $\gamma$ -CD, Bcc, and DeTMA.



where  $K_2$  is the equilibrium constant for the formation of the 1:1:1  $\gamma\text{-CD}$ –Bcc–DeTMA inclusion complex ( $\gamma\text{-CD} \cdot \text{Bcc} \cdot \text{DeTMA}$ ). Under our experimental conditions of low Bcc concentration, the fluorescence intensity of a relevant species is proportional to its concentration. For Bcc solution containing  $\gamma$ -CD and DeTMA, the fluorescence intensity,  $I_f$ , is represented as

$$I_f = b[\text{Bcc}] + c[\gamma\text{-CD} \cdot \text{Bcc}] + d[\gamma\text{-CD} \cdot \text{Bcc} \cdot \text{DeTMA}] \quad (4)$$

Here,  $b$ ,  $c$ , and  $d$  are experimental constants including the fluorescence quantum yields of free Bcc, the 1:1  $\gamma\text{-CD}$ –Bcc inclusion complex, and the 1:1:1  $\gamma\text{-CD}$ –Bcc–DeTMA inclusion complex, respectively. In the absence of  $\gamma$ -CD, the fluorescence intensity of Bcc was found to be quenched by DeTMA. The fluorescence quenching of Bcc in the absence of  $\gamma$ -CD is due to the dynamic quenching by DeTMA, because in the ground state a complex is not formed between Bcc and DeTMA. From the dependence of the fluorescence intensity of Bcc on the DeTMA concentration, the Stern–Volmer constant,  $K_{\text{SV}}$ , was evaluated to be  $11.6 \text{ mol}^{-1} \text{ dm}^3$  (Figure S2). The  $K_{\text{SV}}$  value of Bcc in aqueous solution containing NaBr was found to be  $9.3 \text{ mol}^{-1} \text{ dm}^3$ . Consequently, the fluorescence quenching of Bcc by DeTMA is due partly to a DeTMA cation, although the fluorescence quenching is mainly caused by  $\text{Br}^-$ . Taking account of the fluorescence quenching of free Bcc by DeTMA, eq 4 is rewritten as

$$I_f = b[\text{Bcc}]/(1 + K_{\text{SV}}[\text{DeTMA}]) + c[\gamma\text{-CD} \cdot \text{Bcc}] + d[\gamma\text{-CD} \cdot \text{Bcc} \cdot \text{DeTMA}] \quad (5)$$

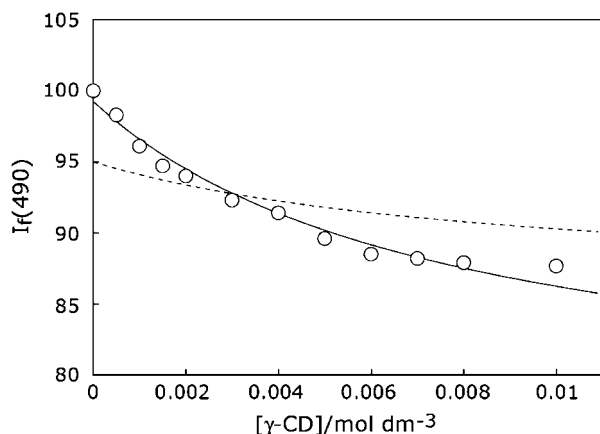


**Figure 8.** Simulation for the observed fluorescence intensities (open circles) of Bcc ( $2.5 \times 10^{-5} \text{ mol dm}^{-3}$ ) in aqueous solutions containing DeTMA ( $5.0 \times 10^{-3} \text{ mol dm}^{-3}$ ) and various concentrations of  $\gamma$ -CD. A best fit simulation curve (solid curve), which has been based on the scheme involving the formation of the 1:1:1  $\gamma$ -CD-Bcc-DeTMA inclusion complex, has been calculated with the evaluated  $K_1$  value ( $110 \text{ mol}^{-1} \text{ dm}^3$ ), the evaluated  $c/b$  value (0.856), an assumed  $K_2$  value of  $35.8 \text{ mol}^{-1} \text{ dm}^3$ , an assumed  $b$  value of  $2.10 \times 10^8 \text{ mol}^{-1} \text{ dm}^3$ , and an assumed  $d$  value of  $0 \text{ mol}^{-1} \text{ dm}^3$ . A best fit simulation curve (dotted curve), which has been based on the scheme not involving the 1:1:1  $\gamma$ -CD-Bcc-DeTMA inclusion complex, has been calculated with the evaluated  $K_1$  value ( $110 \text{ mol}^{-1} \text{ dm}^3$ ), the evaluated  $c'/b'$  value ( $=c/b$ ), and an assumed  $b'$  value of  $2.01 \times 10^8 \text{ mol}^{-1} \text{ dm}^3$ .  $\lambda_{\text{ex}} = 330 \text{ nm}$ .  $\lambda_{\text{obs}} = 490 \text{ nm}$ .

Using the already evaluated  $K_1$  value, the ratio,  $c/b$ , could be estimated to be 0.856 from a simulation of the fluorescence intensity as a function of the  $\gamma$ -CD concentration in  $\gamma$ -CD solution without DeTMA (Figure S3). Introducing the equilibrium constants, eq 5 is given by

$$I_f = \frac{b/(1 + K_{\text{SV}}[\text{DeTMA}]) + cK_1[\gamma\text{-CD}] + dK_1K_2[\gamma\text{-CD}][\text{DeTMA}][\text{Bcc}]_0}{(1 + K_1[\gamma\text{-CD}] + K_1K_2[\gamma\text{-CD}][\text{DeTMA}])} \quad (6)$$

where  $[\text{Bcc}]_0$  is the initial concentration of Bcc. The values of  $c/b$ ,  $K_{\text{SV}}$ , and  $K_1$  have already been evaluated. Thus, we simulated the observed fluorescence intensity for Bcc solution containing  $\gamma$ -CD and DeTMA ( $0.005 \text{ mol dm}^{-3}$ ) as a function of the  $\gamma$ -CD concentration. A best fit simulation curve (solid curve), which has been calculated from eq 6, is shown in Figure 8. The simulation curve reproduces the observed fluorescence intensities. From the simulation, values of  $K_2$ ,  $b$ , and  $d$  are estimated to be 35.8 (Table 1),  $2.10 \times 10^8$ , and  $0 \text{ mol}^{-1} \text{ dm}^3$ , respectively. A  $d$  value of  $0 \text{ mol}^{-1} \text{ dm}^3$  indicates that, within the ternary inclusion complex, DeTMA thoroughly quenches the Bcc fluorescence. This result is reasonable. Because a DeTMA molecule in the ternary inclusion complex is in the neighborhood of a Bcc molecule within the  $\gamma$ -CD cavity, the quenching efficiency is expected to be significantly high. This supports the formation of the 1:1:1  $\gamma$ -CD-Bcc-DeTMA inclusion complex. If the ternary inclusion complex is not formed, the fluorescence intensity for Bcc solution containing  $\gamma$ -CD and DeTMA is represented by

**Table 1.** The  $K_2$  Values of Phen, Phent, and Bcc for TMOA, DeTMA, DoTMA, SDeS, SUnS, and SDoS

|       | $K_2^b/\text{mol}^{-1} \text{ dm}^3$ |                     |                 |
|-------|--------------------------------------|---------------------|-----------------|
|       | Phen                                 | Phent <sup>a)</sup> | Bcc             |
| TMOA  | 380                                  | 30                  | 15              |
| DeTMA | 510                                  | 270                 | 36              |
| DoTMA | 4600                                 | 910                 | 69              |
| SDeS  | 2500                                 | 12                  | — <sup>c)</sup> |
| SUnS  | 5500                                 | 510                 | — <sup>c)</sup> |
| SDoS  | 20000                                | 230                 | — <sup>c)</sup> |

a) In pH 7.3 buffer. b) The errors are less than 30%. c) The  $K_2$  value could not be evaluated because of a small change in the fluorescence intensity.

$$I_f = \frac{b'/(1 + K_{\text{SV}}[\text{DeTMA}]) + c'K_1[\gamma\text{-CD}][\text{Bcc}]_0/(1 + K_1[\gamma\text{-CD}])}{(1 + K_1[\gamma\text{-CD}] + K_1K_2[\gamma\text{-CD}][\text{DeTMA}])} \quad (7)$$

where  $b'$  and  $c'$  are experimental constants including the fluorescence quantum yield of free Bcc and that of the 1:1  $\gamma$ -CD-Bcc inclusion complex, respectively. The value of  $c'/b'$  is equal to the value of  $c/b$  already obtained. A best fit simulation curve (dotted curve), which is based on the scheme of no formation of the ternary inclusion complex, does not fit the observed fluorescence intensity data, supporting the formation of the 1:1:1  $\gamma$ -CD-Bcc-DeTMA inclusion complex (Figure 8).

In tetrakis(4-sulfonatophenyl)porphyrin (TSPP) solution containing  $\gamma$ -CD and TMOA or hexyltrimethylammonium bromide (HTMA), a 1:1:1 ternary inclusion complex is formed among  $\gamma$ -CD, TSPP, and TMOA (or HTMA).<sup>24</sup> As previously described, the formation of a 1:1:1  $\gamma$ -CD-1-pyrenesulfonate-TMOA (or -DeTMA) inclusion complex has been reported.<sup>11</sup> As in the cases of the complexes of  $\gamma$ -CD-TSPP-TMOA (or -HTMA) and  $\gamma$ -CD-1-pyrenesulfonate-TMOA (or -DeTMA), an alkyl chain of DeTMA is likely bound to the  $\gamma$ -CD cavity together with Bcc.

Absorption and fluorescence spectral changes, which are similar to those for DeTMA, respectively, were observed for TMOA and DoTMA (Figures S4–S7). As in the case of DeTMA, ternary inclusion complexes are most likely formed for TMOA and DoTMA. The  $K_2$  values for TMOA and DoTMA were determined to be 14.7 and  $69.3 \text{ mol}^{-1} \text{ dm}^3$ , respectively, from simulations similar to that for DeTMA (Figures S8 and S9). These  $K_2$  values are summarized in Table 1. The  $K_2$  value increases as an alkyl chain in an alkyltrimethylammonium ion is lengthened. The dependence of  $K_2$  on the length of an alkyl chain is similar to that in the system of  $\gamma$ -CD-1-pyrenesulfonate-alkyltrimethylammonium ion.<sup>11</sup>

#### Inclusion Complexes of $\gamma$ -CD with Phent and Phen.

From titration experiments using the absorbance and the fluorescence intensity of Phent, the  $\text{p}K_a$  value and the apparent  $\text{p}K_a^*$  value of Phent have been reported to be 4.62 and 4.66, respectively.<sup>17</sup> Consequently, Phent in pH 7.3 buffer exists in a neutral form. Upon the addition of  $\gamma$ -CD, the absorption bands of Phent in pH 7.3 buffer have been shifted to longer wavelengths, accompanied by a decrease in the absorption-peak intensity (Figure S10). This suggests the formation of an inclusion complex of  $\gamma$ -CD with Phent. The fluorescence

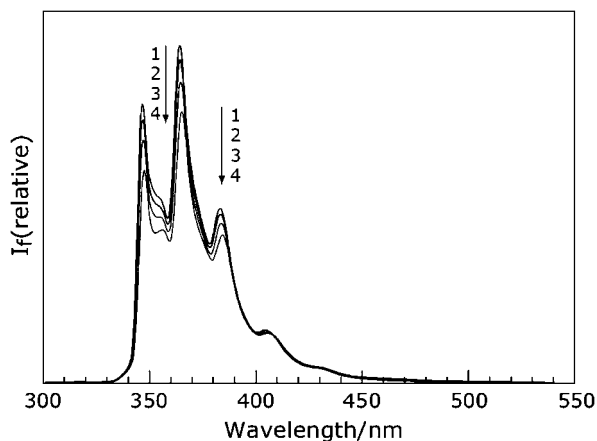


**Figure 9.** Fluorescence spectra of Phent ( $1.2 \times 10^{-6}$  mol dm $^{-3}$ ) in aqueous solutions containing various concentrations of  $\gamma$ -CD. Concentration of  $\gamma$ -CD: (1) 0, (2)  $1.0 \times 10^{-3}$ , (3)  $3.0 \times 10^{-3}$ , and (4)  $1.0 \times 10^{-2}$  mol dm $^{-3}$ .  $\lambda_{\text{ex}} = 290$  nm.

intensity of Phent was reduced by the addition of  $\gamma$ -CD, suggesting the formation of the  $\gamma$ -CD–Phent inclusion complex.<sup>17</sup> From the fluorescence intensity change, the  $K_1$  value for Phent has been evaluated to be  $150 \pm 30$  mol $^{-1}$  dm $^3$ .<sup>17</sup> This  $K_1$  value for Phent in pH 7.3 buffer is slightly greater than that ( $110 \pm 30$  mol $^{-1}$  dm $^3$ ) for Bcc in aqueous solution.

When  $\gamma$ -CD was added to Phent solution, the absorption bands were shifted to longer wavelengths, suggesting the formation of an inclusion complex of  $\gamma$ -CD with Phent (Figure S11). Figure 9 exhibits fluorescence spectra of Phent in aqueous solution containing various concentrations of  $\gamma$ -CD. As the  $\gamma$ -CD concentration is increased, the fluorescence intensity is reduced, accompanied by slight shifts of the fluorescence peaks to longer wavelengths and the sharpening of the bands. The sharpening of the fluorescence bands indicates that a Phent molecule in  $\gamma$ -CD solution is located in a less polar environment. Consequently, these findings indicate the formation of the inclusion complex of  $\gamma$ -CD with Phent. From a double-reciprocal plot, a  $K_1$  value of  $100 \pm 5$  mol $^{-1}$  dm $^3$  has been evaluated for Phent (Figure S12). A straight line well fit to the observed data indicates the formation of the 1:1  $\gamma$ -CD–Phent inclusion complex. This  $K_1$  value for Phent is slightly less than that for Phent.

From the fluorescence intensity change, the  $K_1$  value for the formation of the 1:1  $\beta$ -CD–Phent inclusion complex has been evaluated to be  $600 \pm 30$  mol $^{-1}$  dm $^3$  in this study. The  $K_1$  values of Phent with  $\gamma$ -CD and  $\beta$ -CD have been reported to be  $(7.7 \pm 0.1) \times 10^2$  and  $(1.5 \pm 0.3) \times 10^3$  mol $^{-1}$  dm $^3$ , respectively, which have been evaluated by means of a vaporization-rate method.<sup>18</sup> From the fluorescence intensity change, however, a  $K_1$  value for  $\beta$ -CD has been reported to be  $170$  mol $^{-1}$  dm $^3$ .<sup>19</sup> Because the  $\gamma$ -CD cavity is most likely too wide to accommodate a Phent molecule, the  $K_1$  value for  $\gamma$ -CD is expected to be less than that for  $\beta$ -CD. The  $K_1$  value ( $600 \pm 30$  mol $^{-1}$  dm $^3$ ) evaluated in this study and the reported  $K_1$  value ( $170$  mol $^{-1}$  dm $^3$ ) for  $\beta$ -CD obtained from the fluorescence data suggest that the  $K_1$  value for  $\gamma$ -CD is less than a  $K_1$  value of  $600$  or  $170$  mol $^{-1}$  dm $^3$  for  $\beta$ -CD. Consequently, a  $K_1$

value of  $100 \pm 5$  mol $^{-1}$  dm $^3$  for  $\gamma$ -CD obtained in this study seems to be reasonable, although a large  $K_1$  value has been estimated from the vaporization-rate method. At pH 7.3, the  $K_1$  value of Phent for  $\gamma$ -CD has been evaluated to be  $91 \pm 19$  mol $^{-1}$  dm $^3$  from the fluorescence intensity change. Taking into account the experimental errors, this  $K_1$  value is nearly the same as that ( $100 \pm 5$  mol $^{-1}$  dm $^3$ ) in water without buffer. Consequently, there seems to be little or no effects of buffer (salt) on the  $K_1$  value.

**Ternary Inclusion Complexes of Phent and Phent with Alkyltrimethylammonium Cations.** When TMOA was added to Phent solution containing  $\gamma$ -CD ( $3.0 \times 10^{-3}$  mol dm $^{-3}$ ), the absorption peaks of Phent were shifted to longer wavelengths, suggesting the formation of a ternary inclusion complex of  $\gamma$ -CD with Phent and TMOA (Figure S13). The fluorescence intensity of Phent in aqueous solution containing TMOA was reduced by the addition of  $\gamma$ -CD (Figure S14). Consequently, simulations similar to that for Bcc were made for Phent solutions containing an alkyltrimethylammonium cation as a function of the  $\gamma$ -CD concentration (Figure S15). The  $K_2$  values of Phent evaluated for TMOA, DeTMA, and DoTMA are summarized in Table 1. As in the case of Bcc, the  $K_2$  value of Phent is increased with an increase in the length of an alkyl chain of an alkyltrimethylammonium cation. For the same alkyltrimethylammonium cation, the  $K_2$  value of Phent is greater than that of Bcc. This finding is most likely due to the hydrophobicity of Phent stronger than that of Bcc. In the ternary inclusion complex of  $\gamma$ -CD–Phent–an alkyltrimethylammonium cation, the strong hydrophobicity of Phent may cause the strong interactions of Phent with an alkyl group of the alkyltrimethylammonium cation located within the  $\gamma$ -CD cavity.

The addition of TMOA to Phent solution without  $\gamma$ -CD resulted in no change in the absorption spectrum of Phent. In the presence of  $\gamma$ -CD of  $3.0 \times 10^{-3}$  mol dm $^{-3}$ , the absorption peaks of Phent were shifted to longer wavelengths by the addition of TMOA (Figure S16). This indicates the formation of a ternary inclusion complex of  $\gamma$ -CD, Phent, and TMOA. As in the cases of Bcc and Phent, the  $K_2$  values of Phent were estimated from simulations similar to those for Bcc and Phent, using the fluorescence intensity change (Figure S17). The  $K_2$  values thus obtained are tabulated in Table 1. A trend in the magnitude of the  $K_2$  value of Phent is the same as those of Bcc and Phent; the longer the length of an alkyl chain of an alkyltrimethylammonium cation is, the larger the  $K_2$  value is. For the same alkyltrimethylammonium cation, the  $K_2$  value follows the order Phent > Phent > Bcc. The  $K_2$  value represents a measure of the affinity of the phenanthrene analog to an alkyl group of the alkyltrimethylammonium cation. Because the hydrophobicity is increased on going from Bcc to Phent, the  $K_2$  value is increased in this order, although, in the ternary inclusion complex, the orientation of the aromatic guest within the  $\gamma$ -CD cavity may be slightly different from each other; the entropy changes for the formation of the 1:1:1 inclusion complex are probably not too different for Phent, Phent, and Bcc. In the ternary inclusion complex, a long alkyl chain of an alkyltrimethylammonium cation is tightly bound to the void space within the  $\gamma$ -CD cavity accommodating a guest molecule such as Phent. Consequently, the  $K_2$  value may greatly reflect

the hydrophobicity of the phenanthrene analog. In the formation of the 1:1 inclusion complex of the analog, on the other hand, the  $K_1$  values are not too different from each other due to the loose binding of the analog to the  $\gamma$ -CD cavity.

To confirm the effects of the snug fit of the phenanthrene analog to the CD cavity, we have estimated the  $K_1$  values for  $\beta$ -CD, of which diameter is less than that of  $\gamma$ -CD. As compared to the  $K_1$  value for  $\gamma$ -CD, the  $K_1$  value for  $\beta$ -CD is expected to more strongly depend on the hydrophobicity of a guest; the  $K_1$  value for  $\beta$ -CD is expected to greatly vary with a variation in the hydrophobicity of a guest molecule. In fact, the  $K_1$  values of  $\beta$ -CD for Bcc, Phent, and Phen obtained in this study are  $280 \pm 20$ ,  $370 \pm 10$ , and  $600 \pm 30 \text{ mol}^{-1} \text{ dm}^3$ , respectively (Figure S18). The  $K_1$  value for  $\beta$ -CD varies in a range wider than the  $K_1$  value for  $\gamma$ -CD does. The wide variation of the  $K_1$  value for  $\beta$ -CD reflects the snug fit of the phenanthrene analogs to the  $\beta$ -CD cavity.

**Ternary Inclusion Complexes of Phent and Phen with Alkanesulfonates or an Alkyl Sulfate.** SDeS, SUNS, and SDoS are organic anions, which have a long alkyl chain. When SDeS, SUNS, and SDoS were used instead of the alkyltrimethylammonium cations, absorption and fluorescence spectral changes of Phent (or Phen) were similar to those for the alkyltrimethylammonium cations (Figures S19–S22). Consequently, ternary inclusion complexes of SDeS, SUNS, and SDoS are most likely formed. Thus, we investigated the dependence of the  $K_2$  value on the alkyl-chain length, using the organic anions having a long alkyl chain. In contrast to the organic cations such as TMOA, the organic anions such as SDeS did not quench the fluorescence of the free phenanthrene analogs. In the simulations of evaluating the  $K_2$  value therefore, we did not take into account the dynamic quenching of the fluorescence of free Phent and free Phen by these organic anions. Figure 10 shows the simulation for the observed fluorescence intensity of Phent ( $3.3 \times 10^{-5} \text{ mol dm}^{-3}$ ) in pH 7.3 buffer containing SDoS ( $3.0 \times 10^{-3} \text{ mol dm}^{-3}$ ) and  $\gamma$ -CD. From the simulation, a  $K_2$  value of  $228 \text{ mol}^{-1} \text{ dm}^3$  has been estimated. The results are summarized in Table 1 (Figure S23 for the simulation of the  $\gamma$ -CD–Phen–SDeS system). Except for SUNS in the case of Phent, the  $K_2$  value is increased on going from SDeS to SDoS; the  $K_2$  value is increased with an increase in the length of an alkyl chain. This trend is the same as that for the alkyltrimethylammonium cations. The  $K_2$  value of Phen for the organic anion is greater than that for the alkyltrimethylammonium cation with the same alkyl chain, while the  $K_2$  value of Phent for the organic anion seems to be rather less than that for the alkyltrimethylammonium cation. The reason for the different trends in the  $K_2$  value between Phen and Phent is not clear at present.

As in the cases of Phen and Phent,  $\gamma$ -CD forms 1:1:1 inclusion complexes with 1-pyrenesulfonate and the organic anions such as SDeS.<sup>11</sup> The  $K_2$  values of 1-pyrenesulfonate for the organic anions are two to three orders of magnitude less than those for the organic cations such as DeTMA. For the ternary inclusion complexes of 1-pyrenesulfonate, the electrostatic repulsion between anionic 1-pyrenesulfonate and anionic an alkanesulfonate (SDeS) decelerates the formation of the ternary inclusion complex. On the other hand, Phen and Phent are present in a neutral form. No electrostatic interactions work

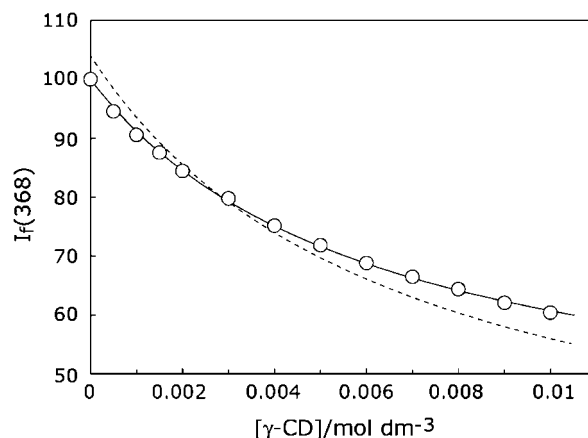


**Figure 10.** Simulation for the observed fluorescence intensities (open circles) of Phent ( $3.3 \times 10^{-5} \text{ mol dm}^{-3}$ ) in pH 7.3 buffer containing SDoS ( $3.0 \times 10^{-3} \text{ mol dm}^{-3}$ ) and various concentrations of  $\gamma$ -CD. A best fit simulation curve (solid curve), which has been based on the scheme involving the formation of the 1:1:1  $\gamma$ -CD–Phent–SDoS inclusion complex, has been calculated with the evaluated  $K_1$  value ( $150 \text{ mol}^{-1} \text{ dm}^3$ ), evaluated  $c/b$  values (0.230), an assumed  $K_2$  value of  $228 \text{ mol}^{-1} \text{ dm}^3$ , an assumed  $b$  value of  $1.00 \times 10^7 \text{ mol}^{-1} \text{ dm}^3$ , and an assumed  $d$  value of  $2.29 \times 10^7 \text{ mol}^{-1} \text{ dm}^3$ . A best fit simulation curve (dotted curve), which has been based on the scheme not involving the formation of the 1:1:1  $\gamma$ -CD–Phent–SDoS inclusion complex, has been calculated with the evaluated  $K_1$  value ( $150 \text{ mol}^{-1} \text{ dm}^3$ ), and  $c'/b'$  value ( $=c/b$ ), and an assumed  $b'$  value of  $1.04 \times 10^6 \text{ mol}^{-1} \text{ dm}^3$ .  $\lambda_{\text{ex}} = 318 \text{ nm}$ .  $\lambda_{\text{obs}} = 368 \text{ nm}$ .

between Phen (Phent) and the organic ions such as SDeS and DeTMA. The  $K_2$  values of Phen for SDeS and SDoS are respectively about four and five times greater than those for DeTMA and DoTMA, which have the same decyl and dodecyl chain as SDeS and SDoS, respectively. The  $K_2$  value of Phent for SDoS is about four times less than that for DoTMA, although the  $K_2$  value of Phent for SDeS is about 22 times less than that for DeTMA. In contrast to the case of 1-pyrenesulfonate,<sup>11</sup> the relatively small difference in the  $K_2$  value between an organic cation and an organic anion may be ascribed to no electrostatic interactions between Phen (Phent) and an organic cation (or organic anion).

### Conclusion

In aqueous solution,  $\gamma$ -CD forms 1:1 inclusion complexes with the phenanthrene analogs (Bcc, Phent, and Phen). The equilibrium constants,  $K_1$ , for the formation of the 1:1  $\gamma$ -CD–phenanthrene analog inclusion complexes are in the range of 100 to  $150 \text{ mol}^{-1} \text{ dm}^3$  for Bcc, Phent, and Phen. On the other hand, the  $K_1$  values for  $\beta$ -CD are in the range of 280 to  $600 \text{ mol}^{-1} \text{ dm}^3$ . This suggests that the fit of a guest to the CD cavity affects the magnitude of the  $K_1$  value for a phenanthrene analog. The 1:1  $\gamma$ -CD–phenanthrene analog inclusion complex further associates with an alkyltrimethylammonium cation, alkanesulfonate, or alkyl sulfate to form a 1:1:1 inclusion complex. The equilibrium constant,  $K_2$ , for the formation of the 1:1:1 inclusion complex is increased with an increase in the

length of an alkyl chain of the alkyltrimethylammonium cation (or alkanesulfonate etc.). In addition, the magnitude of  $K_2$  strongly depends on the kind of the phenanthrene analog, while the magnitude of  $K_1$  is not too different from each other. The  $K_2$  value of Phen for an alkyltrimethylammonium cation is less than that for an organic anion such as alkyl sulfate having an alkyl chain of the same length as that of the alkyltrimethylammonium cation.

### Supporting Information

Titration curve, Stern–Volmer plot, absorption spectra, fluorescence spectra, double-reciprocal plots, and simulations for the fluorescence intensity of Bcc, Phent, and Phen. This material is available free of charge on the web at <http://www.csj.jp/journals/bcsj/>.

### References

- 1 W. Saenger, *Angew. Chem., Int. Ed. Engl.* **1980**, *19*, 344.
- 2 M. L. Bender, M. Komiyama, *Cyclodextrin Chemistry*, Springer-Verlag, New York, **1978**.
- 3 K. A. Connors, *Chem. Rev.* **1997**, *97*, 1325.
- 4 R. J. Clarke, J. H. Coates, S. F. Lincoln, *Carbohydr. Res.* **1984**, *127*, 181.
- 5 H. Hirai, N. Toshima, S. Uenoyama, *Bull. Chem. Soc. Jpn.* **1985**, *58*, 1156.
- 6 R. J. Clarke, J. H. Coates, S. F. Lincoln, *J. Chem. Soc., Faraday Trans. 1* **1986**, *82*, 2333.
- 7 S. Hamai, *Bull. Chem. Soc. Jpn.* **2000**, *73*, 861.
- 8 C. Lee, Y. W. Sung, J. W. Park, *J. Phys. Chem. B* **1999**, *103*, 893.
- 9 S. Hamai, *Bull. Chem. Soc. Jpn.* **2002**, *75*, 2371.
- 10 K. Kano, I. Takenoshita, T. Ogawa, *Chem. Lett.* **1980**, 1035.
- 11 S. Hamai, *J. Inclusion Phenom. Macrocyclic Chem.* **2009**, *63*, 77.
- 12 A. Örstam, J. B. A. Ross, *J. Phys. Chem.* **1987**, *91*, 2739.
- 13 S. Nigam, G. Durocher, *J. Photochem. Photobiol., A* **1997**, *103*, 143.
- 14 S. Santra, S. K. Dogra, *J. Photochem. Photobiol., A* **1996**, *101*, 221.
- 15 Y. C. Guillaume, E. Peyrin, *Anal. Chem.* **1999**, *71*, 2046.
- 16 J. M. Schuette, T. T. Ndou, A. M. de la Pena, S. Mukundan, Jr., I. M. Warner, *J. Am. Chem. Soc.* **1993**, *115*, 292.
- 17 S. Hamai, *Bull. Chem. Soc. Jpn.* **2006**, *79*, 1039.
- 18 I. Sanemasa, T. Takuma, T. Deguchi, *Bull. Chem. Soc. Jpn.* **1989**, *62*, 3098.
- 19 F. J. Alonso, A. Heredia, J. C. Marquez, *J. Mol. Struct.* **1986**, *143*, 399.
- 20 W. H. Melhuish, *J. Phys. Chem.* **1960**, *64*, 762.
- 21 a) H. A. Benesi, J. H. Hildebrand, *J. Am. Chem. Soc.* **1949**, *71*, 2703. b) S. Hamai, *Bull. Chem. Soc. Jpn.* **1982**, *55*, 2721.
- 22 A. Harada, M. Okada, J. Li, M. Kamachi, *Macromolecules* **1995**, *28*, 8406.
- 23 M. Kodaka, *J. Am. Chem. Soc.* **1993**, *115*, 3702.
- 24 S. Hamai, Y. Sasaki, T. Hori, A. Takahashi, *J. Inclusion Phenom. Macrocyclic Chem.* **2006**, *54*, 67.